Kumar et al. 2018. *Int. J. Vehicle Structures & Systems*, 10(4), 282-286
ISSN: 0975-3060 (Print), 0975-3540 (Online)
doi: 10.4273/ijvss.10.4.11

International Journal of Vehicle Structures & Systems
Available online at www.maftree.org/eja

Comparative Approaches for Fatigue Life Estimation of Aluminium Alloy for Aerospace Applications

K. Naveen Kumar[a], R. Vijayanandh[b], G. Raj Kumar, B. Sanjeev, Hariharan Balachander and S. Guru Prasad

Dept. of Aero. Engg., Kumaraguru College of Tech., Coimbatore, Tamil Nadu, India
[a]Corresponding Author, Email: Naveenkumar.k.aeu@kct.ac.in
[b]Email: vijayanandh.raja@gmail.com

ABSTRACT:

The objective of this paper is to estimate the fatigue life behaviour of Al 7075-T6 using experimental and numerical methods for the purpose of aerospace applications. In this paper, initially static properties for the specimens are determined using Universal Testing Machine (UTM) under tensile loading. The cyclic bending load is applied on the material using fatigue test and the dynamic properties are determined. Experimental and numerical studies are carried out to determine the fatigue strength and endurance limit values of aluminium alloy 7075-T6 at different types of loading. The fatigue strength and structural integrity of the aluminium alloy 7075 - T6 are investigated using S-N curve. In numerical simulation, the reference model of this paper has been modelled by CATIA and thereby it is imported into ANSYS workbench 16.2 to investigate the stress distribution and number of cycles to failure of an aluminium alloy 7075-T6 under tensile loading. The mechanical properties are evaluated using both the approaches and finally the comparative study is carried out.

KEYWORDS:

Aluminium alloy 7075-T6; Tensile test; Fatigue test; S-N curve; Endurance limit; Goodman equation

CITATION:

K.N. Kumar, R. Vijayanandh, G.R. Kumar, B. Sanjeev, H. Balachander and S.G. Prasad. 2018. Comparative Approaches for Fatigue Life Estimation of Aluminium Alloy for Aerospace Applications, *Int. J. Vehicle Structures & Systems*, 10(4), 282-286. doi:10.4273/ijvss.10.4.11.

NOMENCLATURE:

$\varepsilon_e \varepsilon_e$	Elastic component of the cyclic strain amplitude
$\sigma_a \sigma_a$	Cyclic stress amplitude
$\sigma_f' \sigma_f'$	Fatigue strength coefficient
$N_f N_f$	Number of cycles to failure
bb	Fatigue strength exponent

1. Introduction

High strength alloys are one of the main utilizers in the aerospace and automobile industry because of their significant weight savings and enhanced performance. Light-weight and high-strength aluminium alloys such as 7075-T6 are most cost effective and widely used in aircraft fuselage and wings and also in automobile industries[1]. In this paper aluminium alloy 7075-T6 has been selected for mechanical characterization. It has 5.16.1% zinc, 2.12.9% magnesium, 1.22.0% copper, and less than half a percentage of silicon, iron, manganese, titanium, chromium, and other metals [2], in which the aircraft manufacturers use aluminium alloy in order to strengthen the aircraft structures. The fatigue life of alloys are based on large number of variables in which state of stress, mode of cycling, and environmental conditions play a prime role [3]. The fatigue process consists of crack initiation and crack propagation to failure. Crack initiation behaviour is the base for the crack growth predictions in a unified approach for fatigue life predictions. Fatigue cracking is one of the primary damage mechanisms of alloys/metals [4]. Today, structural fatigue has assumed an even greater importance as a result of the ever-increasing use of high-strength materials and the desire for higher performance from these materials. There are three basic factors necessary to cause fatigue [5]: (1) a maximum tensile stress of sufficiently high value, (2) a huge enough fluctuation in the applied stress, and (3) a huge number of cycles of the applied stress. After a certain amount of cycles, cracks start to form in the high stress concentration areas [6]. Halit et al [7] investigated the mechanical behaviour of AA 7075-T6 during cyclic loading to improve the strength.

Increasing the strength of aluminium can be achieved in a moderate way by work hardening and, to a substantial extent, by precipitation hardening combined with mechanical and thermal treatments. Newman et al [8] studied the fatigue and crack-growth analyses on 7075-T651 aluminium alloy coupons under constant and variable-amplitude loading to identify the failure mechanisms of 7075-T651. The experimental work on fatigue damage mechanisms in fibre reinforced with alumina oxide composites under cyclic reversed (fully reversible tension-compression loads) loading is examined and the failure mechanisms of alloy specimen is identified using scanning electron microscope [9]. Based on the above mentioned literature study, the

tensile test and fatigue test of aluminium 7075 is performed to determine the stress values, and to determine its finite element ductile fracture criterion according to a simulation analysis.

2. Experimental analysis

The specimen for tensile test has been prepared as per the ASTM standard D 3039-76, in which the size 300mm × 20mm × 10mm are followed for the Al alloys as shown in Fig. 1 and the conceptual design has been modelled using CATIA for numerical analysis which has been shown in the Fig. 2.

Fig. 1: Tensile test specimen dimension in mm

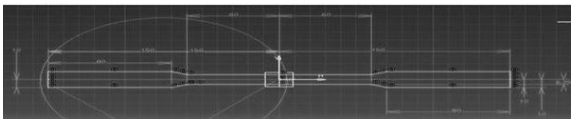

Fig. 2: Tensile test specimen dimension in mm

The tensile and fatigue tests are carried out, according to the ASTM specifications for Al 7075-T6 specimens. The specimens are subjected to uni-axial tension using 100kN Servo Hydraulic Universal Testing Machine [10]. The dog-bone type and the straight-side type with end tabs are commonly used for tensile test according to ASTM standard D 3039-76, the whole test setup as shown in Fig. 3.

Fig. 3: Universal testing machine with magnification for tensile test

During the test, a uni-axial load is applied through both the ends of the specimen and then the results are analysed to calculate the tensile strength of specimens. ASTM standard D3479-76 standard fatigue specimen of size 150mm × 20mm × 10mm are prepared from the Al alloys are shown in Fig. 4. Two different types of specimens are formed to dog-bone shaped with total thickness 10mm according to ASTM standard D3479-76, to determine the fatigue strength with more confirmation. The dog-bone specimen of suitable dimensions have to be cut using a diamond cutter to avoid machining defects and maintain good surface finish for fatigue test from the Al alloys.

Fig. 4: Fatigue test specimen dimension in mm

Fig. 5: Fatigue testing machine with specimen for fatigue test

The fatigue testing machine type 6,301 as shown in Fig. 5 used to test the Al specimen and calculate the number of cycles to failure. The power of motor (0.5 HP) is connected along with the testing unit. The grips are provided for bend test where the load is applied at both ends of the specimen by an oscillating spindle motor. Then the motor is started on to the fatigue, the specimen attains fracture after long time. The revolution counter is fixed to the motor to record the number of cycles; the cycling rate is 1,420 rpm [11]. The number of cycles required for attaining fatigue fracture and fatigue life is calculated using [12-13],

$$\varepsilon_e = \frac{\sigma_a}{E} = \frac{\sigma_f'}{E} \times \left(2N_f\right)^b \quad (1)$$

Fatigue load history, as determined by testing with rotating bend tests, provides information about mean and alternating stress. The rate of crack propagation in tests has been shown to be related to the stress ratio of the load cycle, and the load's mean stress [14]. Cracks only propagate under tensile loads. For that reason, if the load cycle induces compressive stress in the area of the crack, it will not produce more damage. However, if the mean stress shows that the complete stress cycle is tensile, the whole cycle will cause damage. Many service load histories will have a non-zero mean stress [15].

The following mean stress correction methods have been developed to eliminate the burden of having to carry out fatigue tests at different mean stresses:

- Goodman method: Generally suitable for brittle materials

$$\frac{\sigma_a}{S_e} + \frac{\sigma_m}{S_u} = 1 \quad (2)$$

- Gerber method: Generally suitable for ductile materials

$$\frac{\sigma_a}{S_e} + \frac{\sigma_m^2}{S_u} = 1 \quad (3)$$

- Soderberg method: Generally the most conservative

$$\frac{\sigma_a}{S_e} + \frac{\sigma_m}{S_y} = 1 \quad (4)$$

All these three methods apply only when all associated S-N curves are based on fully reversed loading. Moreover, these corrections only become significant if the applied fatigue load cycles have large mean stresses compared to the stress range [16]. Uni-axial tension has been applied to the test specimens, in which the load rate is set at 0.5kN/min. The relationship between the applied load and the displacement is linear until the test specimen failure. Table 1 contains the experimental results of ultimate load and ultimate stress for three different test specimens that have been undergone the tensile test. Observation from the experimental is noted in which yield stress is 553.23MPa and Young's modulus is 71.1GPa play a vital role.

Table 1: Experimental results

Specimen	Ultimate load, kN	Ultimate stress, MPa
1	76.6	624.11
2	75.5	620.24
3	76.0	622.22

Stress-life and strain-life methods are often used based on the stabilized stress-strain hysteresis loops. Crack initiation analyses are used to simulate the total fatigue life (S-N) of aluminium specimens made of 7075-T6 and tested under constant amplitude loading. The fatigue process consists of crack initiation and crack propagation to failure. New high strength alloys often have small critical flaw sizes and as a result, most lifetime of the structures made from these alloys is spent in initiating fatigue cracks [17-20]. The fatigue tests are done in the laboratory. The fatigue machine performs the fatigue tests under cyclic reversed loading with stress ratio R and also S-N data is used to predict the fatigue behaviour of the Al alloy specimen [21] as shown in the Fig. 6. Crack initiation, micro crack growth and fatigue growth are the three regions of the damage behaviour.

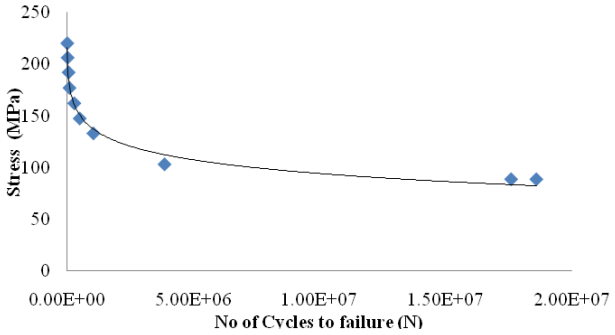

Fig. 6: Experimental results of S-N curve for Al alloy

In the crack initiation region, the development process of the damage is not inducted with initial cyclic loading because Aluminium alloy is perfectly obeys the elastic manner. Due to reversed cyclic loading affect the initial damage in the Aluminium alloy, which occurs below the 2×10^5 cycles [22]. The micro crack growth, fatigue crack growth region is continuously monitored during the fatigue test. The applied cyclic load level is the only key parameter to evaluate the failure damage mechanism and fatigue crack growth. In fatigue growth region, the failure load above 10^5 cycles is expected to produce the damage to the fracture within an infinitely long time and, hence underneath the Al alloy specimen for an expected endurance limit [23] using S-N data as shown in Fig. 6. From the experimental data collected, it can be inferred that the stress values increases 33% in between the range of 150 to 200kg and the number of cycles to failure reduces 88% [24]. The endurance limit determined from the graph value is 87.31MPa.

3. Finite element analysis (FEA)

Goodman equation is used to estimate the endurance limit using the FEA stress results. Boundary conditions are predominant for structural simulations due to its result initialization property. In this paper boundary conditions for both ends of the specimen were given as fixed end boundary conditions and midpoint bending load of magnitudes from 200kg to 375kg in steps of 25kg are given and analysis are carried out separately [25]. Fig. 7 shows the conceptual design of fatigue test specimen, which has been implemented in the structural simulation and thereby the stress and fatigue life has been analysed for various loading with the given tensile boundary conditions. Figs. 8 to 15 show the predicted von mises stress and life estimation variation of Al7075-T6 for loads of 200kg, 250kg, 300kg and 375kg. From the numerical data, the same effect of stress increment and number of cycle reduction as observed in experimental analysis is achieved in the same loading conditions.

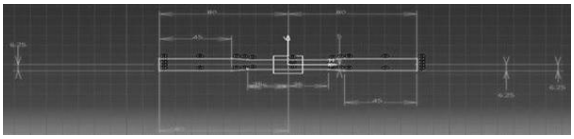

Fig. 7: Fatigue test specimen dimension in mm

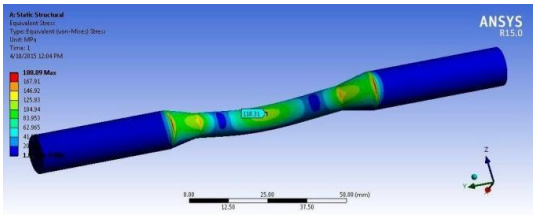

Fig. 8: Stress plot for 200 kg

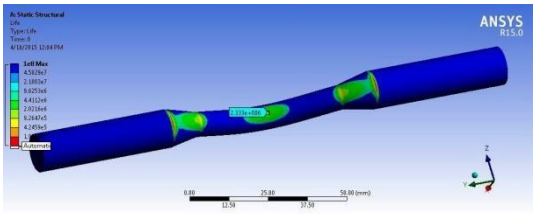

Fig. 9: Life plot for 200 kg

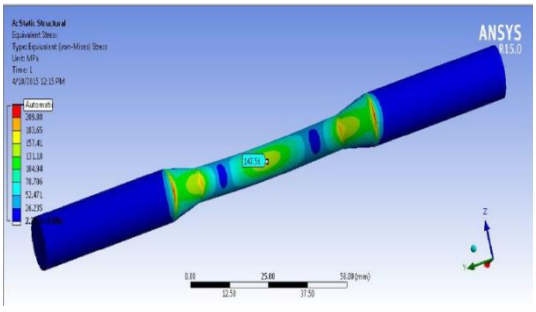

Fig. 10: Stress variation for 250 kg

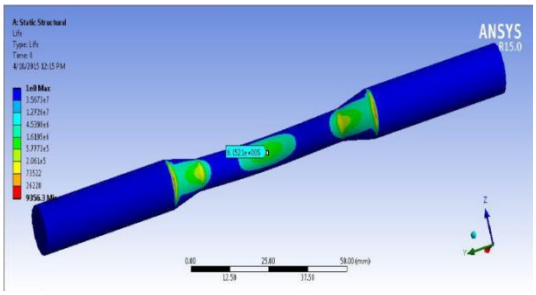

Fig. 11: Life variation for 250 kg

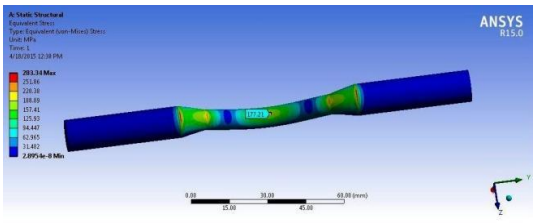

Fig. 12: Stress plot for 300 kg

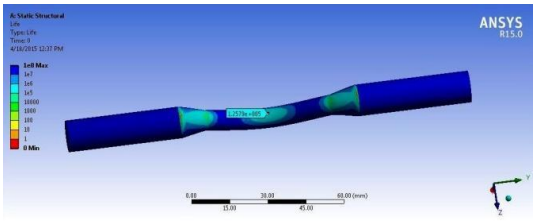

Fig. 13: Life plot for 300 kg

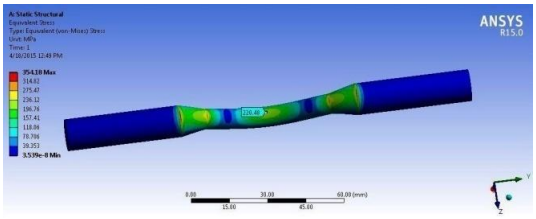

Fig. 14: Stress plot for 375 kg

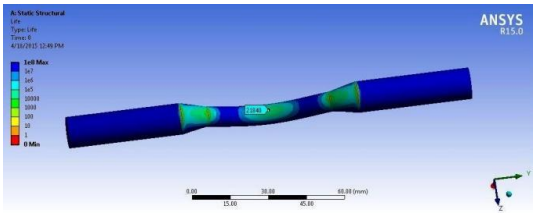

Fig. 15: Life plot for 375 kg

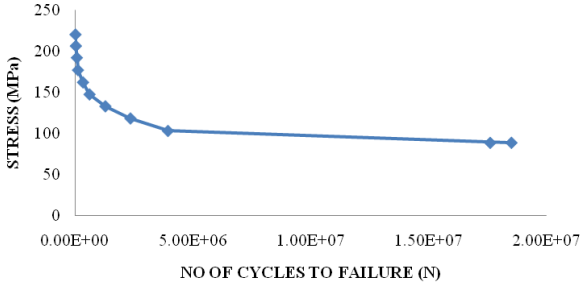

Fig. 16: Numerical results of S-N curve for Al alloy

Fig. 16 explains the relationship between the number of cycles to failure and stress, which have been analysed from FEA. The endurance limit achieved by the numerical data is 93.62MPa. The detailed mechanical property and withstanding fatigue capability analysis of Aluminium Alloy 7075-T6 has been carried out for both the approaches and presented in Table 2. Both the results are perfectly suited for aerospace structures and underwent the tensile as well as cyclic loading.

Table 2: S-N curve – Experiment vs. FEA

Load		Experimental results		FEA results	
kg	N	Stress (MPa)	No. of cycles to failure	Stress (MPa)	No. of cycles to failure
150	1471.50	88.559	1.76×10^{7}	88.559	18503426
175	1716.75	103.06	3.87×10^{6}	103.06	3949256
200	1962	118.31	2.06×10^{6}	118.31	2343327
225	2207.25	133.07	1.05×10^{6}	133.07	1290942
250	2452.5	147.56	5.1×10^{5}	147.56	615212
275	2697.75	162.32	2.95×10^{5}	162.32	339731
300	2943	177.21	1.05×10^{5}	177.21	125791
325	3188.25	192.33	7.02×10^{4}	192.33	79128
350	3433.50	206.57	3.01×10^{4}	206.57	34877
375	3678.75	220.57	1.73×10^{4}	220.48	21840

4. Conclusion

This purpose of this work is to predict the fatigue strength of Al alloy specimens using fatigue test and ANSYS FEA under fatigue for different types of loadings. The Al alloy specimens were modelled and simulated to show the performance improvement of fatigue strength using ANSYS FEA. Experimental and numerical data showed that the maximum stress occurred at the dog bone areas of specimens, whereas minimum displacement occurred at 0.2mm compared to 0.4mm. From the von mises stresses results, the FEA produced higher results than experimental test of Al specimens. The error percentage of endurance limit between FEA and experiment analysis was calculated to be within 5%. The reason might be due to manual errors such as finishing of the specimens, its improper fitting to the machine during testing and this much variation in numerical analysis is acceptable.

REFERENCES:

[1] J.F. Tu and A.G. Paleocrassas. 2011. Fatigue crack fusion in thin-sheet aluminum alloys AA7075-T6 using low-speed fibre laser welding, *J. Materials Processing Tech.*, 211, 95-102. https://doi.org/10.1016/j.jmatprotec. 2010. 09.001.

[2] K.N. Kumar, R. Vijayanandh, M.S. Kumar, G.R. Kumar and M. Bak. 2017. Experimental and numerical analysis on fatigue life of aluminium alloy 7075-T6, *Proc. Int. Conf. in Recent Innovations in Production Engg.*, MIT, Chennai.

[3] R.H. Oskouei and R.N. Ibrahim. 2012. The effect of clamping compressive stresses on the fatigue life of Al 7075-T6 bolted plates at different temperatures, *Materials and Design*, 34, 90-97. https://doi.org/10. 1016/j.matdes.2011.07.073.

[4] A.B. Harman and A.N. Rider. 2013. On the fatigue durability of clad 7075-T6 aluminium alloy bonded joints representative of aircraft repair, *Int. J. Adhesion and Adhesives*, 44, 144-156. https://doi.org/10.1016/j. ijadhadh.2013.01.009.

[5] F. Benyahia, L. Aminallah, A. Albedah, B.B. Bouiadjra and T. Achour. 2015. Experimental and numerical analysis of bonded composite patch repair in aluminum

alloy 7075 T6, *Materials and Design*, 73, 67-73. https://doi.org/10.1016/j.matdes.2015.02.009.

[6] R.H. Oskouei and R.N. Ibrahim. 2012. An investigation on the fatigue behaviour of Al 7075-T6 coated with titanium nitride using physical vapour deposition process, *Materials and Design*, 39, 294-302. https://doi.org/10.1016/j.matdes.2012.02.056.

[7] H.S. Turkmen, R.E. Loge, P.R. Dawson and M.P. Miller. 2003. On the mechanical behaviour of AA 7075-T6 during cyclic loading, *Int. J. Fatigue*, 25, 267-281. https://doi.org/10.1016/S0142-1123(02)00149-4.

[8] J.C. Newman, E.L. Anagnostou and D. Rusk. 2014. Fatigue and crack-growth analyses on 7075-T651 aluminum alloy coupons under constant and variable-amplitude loading, *Int. J. Fatigue*, 62, 133-143. https://doi.org/10.1016/j.ijfatigue.2013.04.020.

[9] H. Taghizadeh, T.N. Chakherlou, H. Ghorbani and A. Mohammadpour. 2015. Prediction of fatigue life in cold expanded fastener holes subjected to bolt tightening in Al alloy 7075-T6 plate, *Int. J. Mech. Sci*., 90, 6-15. https://doi.org/10.1016/j.ijmecsci.2014.10.026.

[10] E. Zalnezhad and A.A.D. Sarhan. 2014. A fuzzy logic predictive model for better surface roughness of Ti-Ti N coating on AL7075-T6 alloy for longer fretting fatigue life, *Measurement*, 49, 256-265. https://doi.org/10.1016/j.measurement.2013.11.042.

[11] T. Zhao and Y. Jiang. 2008. Fatigue of 7075-T651 aluminium alloy, *Int. J. Fatigue*, 30, 834-849. https://doi.org/10.1016/j.ijfatigue.2007.07.005.

[12] E. Donnelly and D. Nelson.2002. A study of small crack growth in aluminium alloy 7075-T6, *Int. J. Fatigue*, 24 1175-89. https://doi.org/10.1016/S01421123(02)00025-7.

[13] S.Q. Hou, X.J. Cai and J.Q. Xu. 2015. A life evaluation formula for high cycle fatigue under uniaxial and multi axial loadings with mean stresses, *Int. J. Mech. Sci*., 93, 229-239. https://doi.org/10.1016/j.ijmecsci.2015.02.002.

[14] D.C. Chen, C.S. You and F.Y. Gao. 2014. Analysis and experiment of 7075 aluminium alloy tensile test, *Proc. Engg*., 81, 1252-1258. https://doi.org/10.1016/j.proeng.2014.10.106.

[15] S.R. Shinde, C.B. Elliott and D.W. Hoeppner. 2007. Quantitative analysis of fretting fatigue degradation in 7075-T6 aluminium alloy, *Tribology Int.*, 40, 542-547. https://doi.org/10.1016/j.triboint.2006.05.009.

[16] J. Muthu. 2014. Fatigue life of 7075-T6 aluminium alloy under fretting condition, *Theoretical and Applied Fracture Mechanics*, 74, 200-208. https://doi.org/10.1016/j.tafmec.2014.09.006.

[17] T.J Harrison, B.R Crawford, M. Janardhana and G. Clark. 2011. Differing microstructural properties of 7075-T6 sheet and 7075-T651 extruded aluminium alloy, *Proc. Engg*., 10, 3117-3121. https://doi.org/10.1016/j.proeng.2011.04.516.

[18] H.E. Misak, V.Y. Perel, V. Sabelkin and S. Mall. 2013. Crack growth behaviour of 7075-T6 under biaxial tension-tension fatigue, *Int. J. Fatigue*, 55, 158-165. https://doi.org/10.1016/j.ijfatigue.2013.06.003.

[19] H.E. Misak, V.Y. Perel, V. Sabelkin and S. Mall. 2013. Corrosion fatigue crack growth behaviour of 7075-T6 under biaxial tension-tension cyclic loading condition, *Engg. Fracture Mechanics*, 106, 38-48. https://doi.org/10.1016/j.engfracmech.2013.04.004.

[20] M.A. Rahmat, R.N. Ibrahim and R.H. Oskouei. 2014. A study on the combined effect of notch and fretting on the fatigue life behaviour of Al 7075-T6, *Materials and Design*, 60, 136-145.

[21] S.M. Kumar, R. Pramod, M.E.S. Kumar and H.K. Govindaraju. 2014. Evaluation of fracture toughness and mechanical properties of aluminium alloy 7075, T6 with nickel coating, *Proc. Engg.*, 97, 178-185.

[22] C. Sun, Z. Lei and Y. Hong. 2014. Effects of stress ratio on crack growth rate and fatigue strength for high cycle and very-high-cycle fatigue of metallic materials, *Mechanics of Materials*, 69, 227-236. https://doi.org/10.1016/j.mechmat.2013.10.007.

[23] C.M. Abreu, M.J. Cristóbal, R. Figueroa and G. Pena. 2015. Wear and corrosion performance of two different tempers (T6 andT73) of AA7075 aluminium alloy after nitrogen implantation, *Applied Surface Sci.*, 327, 51-61. https://doi.org/10.1016/j.apsusc.2014.11.111.

[24] R. Vijayanandh, G.R. Kumar, M.S. Kumar, M. Karthick and T. Ramganesh. 2016. Fatigue life estimation of aircraft engine compressor with suitable material selection, *Proc. 10th Int. Conf. Intelligent Systems and Control*, Coimbatore, India. https://doi.org/10.1109/ISCO.2016.7727055.

[25] G.R. Kumar, R. Vijayanandh, M.S. Kumar and S.S. Kumar. 2017. Experimental testing and numerical simulation on natural composite for aerospace applications, *Proc. 2nd Int. Conf. Condensed Matter & Applied Physics*, Bikaner, Rajasthan, India. https://doi.org/10.1063/1.5032892.